Journal of Seismology **6:** 379–396, 2002.

Attenuation characteristics of peak ground acceleration from fault trace of the 1999 Kocaeli (Turkey) earthquake and comparison of spectral acceleration with seismic design code

Yoshimitsu Fukushima[1], Onur Köse[2], Tekin Yürür[2], Philippe Volant[3], Edward Cushing[3] & Richard Guillande[4]
[1]*Izumi Research Institute, Shimizu Corporation, Japan;* [2]*Hacettepe University, Department of Geological Engineering, Remote Sensing Laboratory, 06532 Ankara, Turkey;* [3]*Institute de Protection et de Surete Nucleaire, France;* [4]*Geosciences Consultants, France*

Received 26 March 2001; accepted in revised form 6 August 2001

Key words: attenuation, design code, ground acceleration, Kocaeli earthquake, spectral acceleration

Abstract

The 17 August 1999 Kocaeli earthquake in Turkey produced a major surface rupture. We traced this surface rupture from Gölcük to Düzce and located it accurately by using GPS. The closest distance from the surface rupture to the strong motion observation sites were determined. Then the attenuation characteristics of the observed peak ground acceleration were compared with the attenuation relation given by Fukushima and Tanaka (1992), which is suitable for the near-fault zone in Japan and gives results that closely match data recorded during the 1995 Hyogo-ken Nanbu earthquake in Japan. Although this attenuation relation was developed for Japan, we found that it agreed well with the KOCAELI earthquake. Furthermore, the observed spectral acceleration of 5% damping was compared with the building design code of Turkey and the observed level was lower than the code.

Introduction

The Kocaeli, Turkey earthquake occurred on 17 August 1999 at 00:01:39.80 (UTC), 03:01:37 a.m. local time. The moment magnitude Mw was 7.4 according to the USGS and Bogaziçi University. The hypocenter, also determined by the USGS, was 40.702N, 29.987E and the focal depth was 17 km. The mechanism of the main event and the aftershock distribution are shown in Figure 1. The earthquake was almost a pure right lateral strike slip, and the aftershock distribution indicates that the rupture was located toward the western end of the North Anatolian Fault Zone. Yagi and Kikuchi (1999) determined a fault model, using far field and strong ground motion records, with the following parameters: Mo = 1.7×10^{20}Mm, source time = 27 sec, fault length and width = 70 km $\times$ 15 km, maximum slip = 7.2 m, and rupture velocity = 2.5 km/s. They concluded that there were two major slips west and east of rupture initiation, with a rupture velocity of 3.2 km/s. The western segment ruptured for 9 seconds following initiation, while rupture on the eastern segment began 7 seconds after the event began. Sekiguchi and Iwata (1999) inverted the dislocation distribution on the fault using strong motion records taken up to a source distance of 350 km, and the fault length was determined to be 70–80 km. This study also indicated two asperities, one on each side of initiation. Koketsu and Komiyama (1999) point out that the recorded peak ground acceleration agrees well with the attenuation relation given by Fukushima and Tanaka (1990). Further, they indicate that if the rupture went towards the surface obliquely, the fault parallel component was not small even for the strike slip. Kagawa (1999) assumed an inhomogeneous rupture model and simulated the strong ground motion using a stochastic Green's function method. The fault length and width were assumed to be 150 km and 24 km, respectively. Here, three asperities were assumed according to the location of large dislocations on the surface. Fairly good agree-

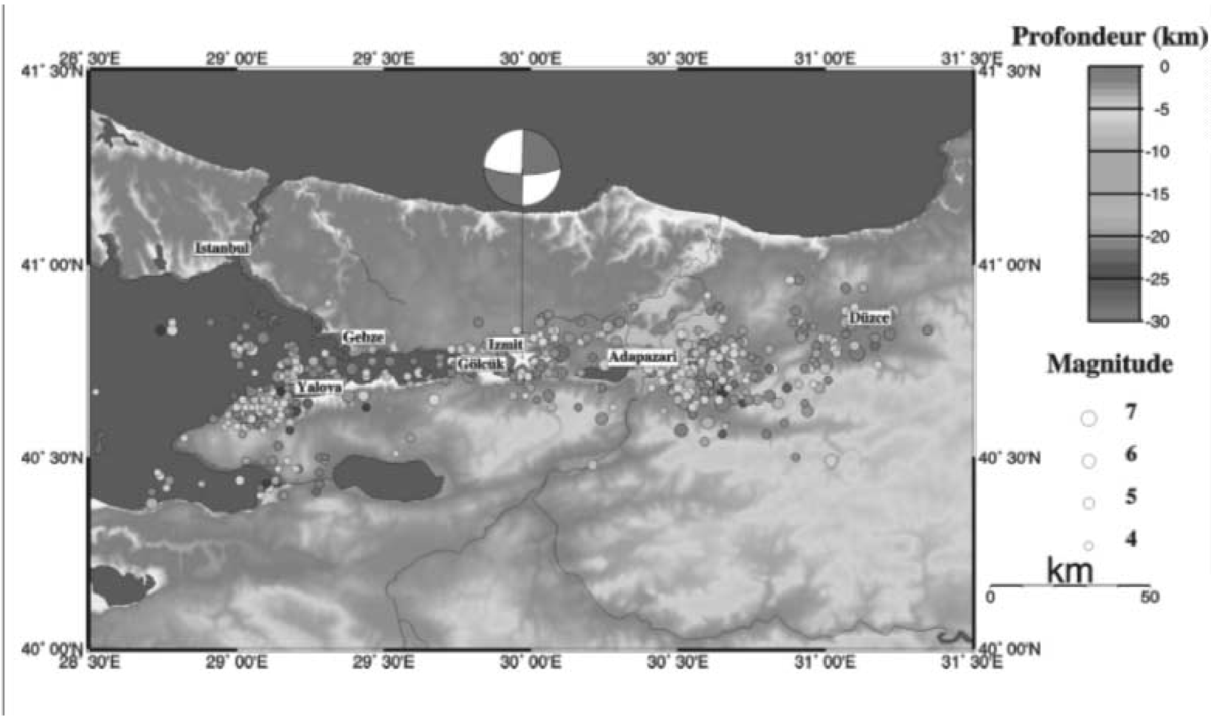

Figure 1. Mechanism of main shock and aftershock distribution.

ment can be seen between the simulated and observed records, though the effect of surface geology is still unclear. Kudo et al. (1999) determined the surface geology in the area of the source using array measurements of micro tremors. They determined S-wave velocity models by inverting the dispersive Rayleigh wave and introduced a large and long-duration strong motion record related to the low S-wave velocity of 200 m/s.

Although the observed data have been compared with several attenuation equations (Earthquake Spectra, 2000, 1999 Kocaeli, Turkey, Earthquake Reconnaissance Report), we would like to compare them with the attenuation relation of Fukushima and Tanaka (1992), which agreed well with the observed data of the 1995 Hyogo-ken Nanbu (Kobe) earthquake (Fukushima et al., 2000). The closest distance from the rupture is an important parameter for the estimation of ground motion, therefore, we inspected the fault trace in the source area and determined the closest distance from the trace.

Surface trace

We followed the surface trace of the rupture from Gölcük to Düzce, in the western section of the North Anatolian Fault Zone. Table 1 indicates the position of the surface rupture as measured by GPS and its dislocations. These points are shown in Figure 2, in which the trace direction is shown by arrows. Photo 1 shows the right lateral dislocation at Gölcük measuring approximately 4m. Shore protection work has been clearly dislocated. East of Gölcük, large vertical settlement was seen, as shown in Photo 2. The dislocation appears to be greater than 2m, as measured against the people photographed, even though the mechanism was almost pure strike slip. Further, the fault divided into several lines with vertical displacement, and as a consequence a town sank into the sea. At the eastern end of Izmit bay, right lateral slip can again be clearly seen, as shown in Photo 3.

The curious thing is that even ordinary houses right beside the fault were able to survive during the earthquake. This was similar to the experience of the 1995 Hyogo-ken Nanbu event, when an ordinary house survived even though the enclosing fence was destroyed by dislocation of the fault trace.

Table 1. Position of surface rupture as measured by GPS and its dislocations

Station no.	Latitude	Longitude	Remarks
1	N40d43m35s	E29d47m57s	dislocation of about 4 m beside the coast in Gölcük.
2	N40d43m16s	E29d56m13s	about 1.5 m of displacement south of Izmit.
3	N40d43m07s	E30d07m38s	dislocation of 2.5 m. Divided tree was found.
4	N40d44m04s	E30d12m31s	landslide Esme.
5	N40d42m47s	E30d19m49s	continuously chased from Arifiye, the fault splits to several cracks.
6	N40d42m32s	E30d22m30s	dislocation of 4.3 m in Arifiye.
7	N40d41m57s	E30d30m10s	dislocation of about 2 m, N275d.
8	N40d42m30s	E30d44m24s	dislocation of 45 cm.
9	N40d43m43s	E30d49m31s	dislocation of 0.66 m, Karadere, Direction: N78.
10	N40d43m45s	E30d50m44s	right lateral strike slip, 5 cm (0.05 m), on a splashing line intersecting the main faulting, located at south of main faulting, south of Karadere.
11	N40d44m53s	E30d51m50s	right lateral strike slip, 5 cm (0.05 m), on a splashing line intersecting the main faulting, located at north of main faulting, north east of Karadere, location: Muhapdede türbe (tomb).
12	N40d45m41s	E30d55m49s	dislocation of 20 cm+28 cm=0.48 m, north of Cayköy in Aksu Valley.
13	N40d46m19s	E30d59m51s	dislocation of 0.07 m (7 cm), Center of Gölyaka, Kasapoglu et al. (1999).
14	N40d46m26s	E31d01m18s	dislocation of 0.03 m (1–3 cm), left lateral strike slip where faulting ends, north of Haciyakup, west of lake Eften.

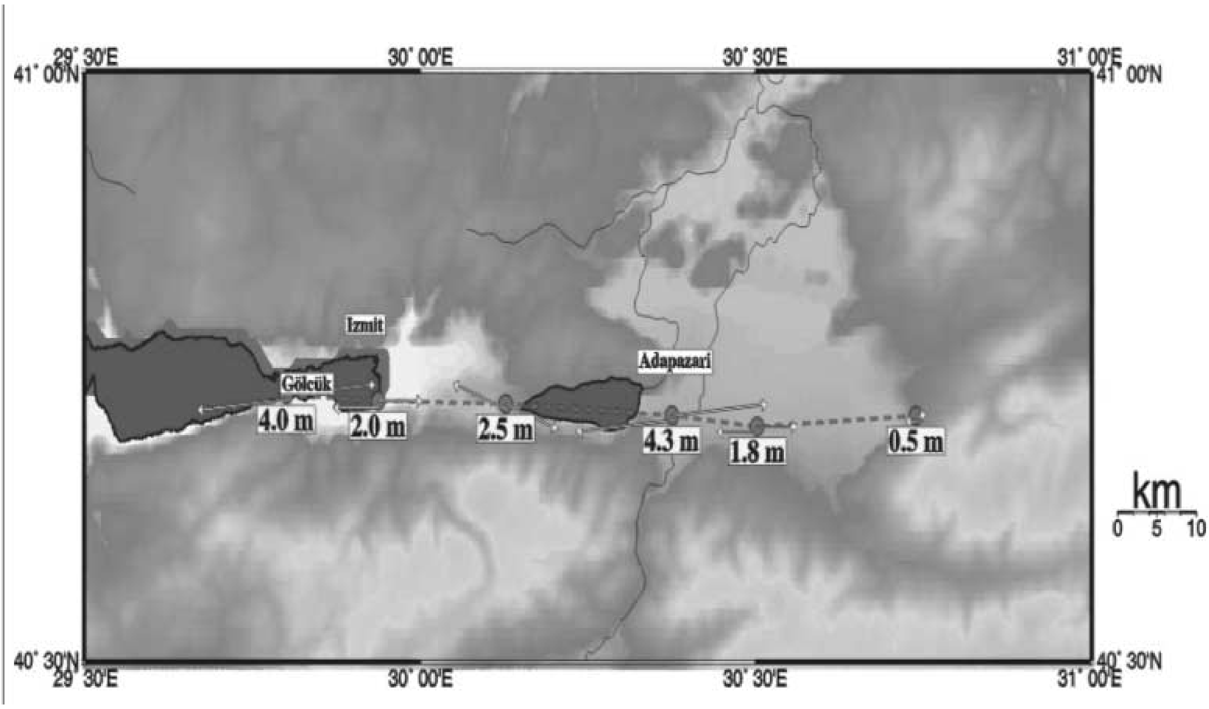

Figure 2. Approximate fault trace and dislocations. Points indicate where surface ruptures were confirmed.

Photo 1. Right lateral dislocation in Gölcük.

The arrows indicating slip direction at Gölcük and Izmit seem to be shifted in Figure 2, and vertical settlement occurred in the tensional field between the two surface traces of right lateral slips. East of Izmit, the fault rupture split again into two lines and the ground between them sank. West of Sapanca lake, the fault trace strikes immediately under a tree, and the trunk was split into two parts which became separated by about 80 cm, as shown in Photo 4. Near this tree, a dislocation of 2 m was measured. East of Sapanca lake, a fence moved 4.3 m horizontally, as shown in Photo 5. Within the limited extent of our investigation, this dislocation was found to be the greatest and it is located just few kilometers south of the very heavily damaged city of Adapazari. Dislocation decreases toward the east, but right lateral slip was found at the eastern end of the Sakarya basin, as shown in Photo 6 where there is a 45 cm dislocation of a fence. Further, the dislocation could be followed right up to Eften lake. Photo 7 indicates one example near Gölyaka where the surface trace is visible even though the displacement is small. A further large event occurred on 12 November 1999 and the new surface rupture was investigated. In Figure 3, the surface ruptures of the events of 17 August and 12 November are shown. It can be imagined that the border between these events was around the small lake near Gölyaka.

The western end is less clear because it is offshore. The aftershocks are distributed beyond Yalova in Figure 1. However, the fringes of the interferogram (Figure 4, CNES/QTISRadar system Dpt., http://www.cnes.fr/cnes/actualites/turquie/images.htm), prepared from co-seismic images of radar satellites acquired before-and-after the earthquake, indicate no dislocation over the eastern peninsula of Yalova. In the case of the 1995 Hyogo-ken Nanbu earthquake in Japan, there was no surface trace on Honshu, the main island, but there are faults along the aftershock belt below Kobe. As with Kocaeli, the presence of existing faults along the aftershock distribution cannot be ignored.

Strong motion records

Strong motion observations were made by Bogaziçi University and the General Directorate of Dis-

Photo 2. Vertical dislocation in Gölcük.

aster Affairs (http://kandilli.koc.net/earthquake.htm, http://angora.deprem.gov.tr/recentquakes.htm), and their records have been made available in digital form on web sites. The maximum peak ground accelerations of the two horizontal components are shown in Table 2 and Figure 5. The sites marked in red are those belonging to the General Directorate of Disaster Affairs, and these are distributed throughout Turkey, while the yellow ones are those of Bogaziçi University in the source region. Peak accelerations seem to increase toward the east, and this perhaps indicates a forward directivity according to the rupture initiated at Izmit.

One of the strong motion observation stations run by Bogaziçi University is shown in Photo 8. The instruments are placed on the foundation of this red building as shown in Photo 9. We determined the closest distance from an assumed fault model to the site as shown in Figure 6. The eastern end of the model is the boundary with the event of 12 November. The western end is assumed to be the edge of the aftershock area.

Attenuation relation

Fukushima and Tanaka (1990) collected a great deal of peak horizontal acceleration (PHA) data and used them to develop an attenuation relation using a two-step regression analysis. Later, new data were added and the attenuation relation was updated, though the new result was little changed from the previous one (Fukushima and Tanaka, 1992). The relation is given in the form of the following equation:

$$\mathrm{Log(PHA)} = 0.42\ \mathrm{Mw} - \log[\mathrm{R}+0.025*10**(0.42\ \mathrm{Mw})] - 0.0033\ \mathrm{R}+1.22 - 0.14\ \mathrm{L} \qquad (1)$$

where, PHA is the mean of the peak accelerations of the two horizontal components in cm/s/s, Mw is the moment magnitude, and R is the closest distance from the fault plane to the site in kilometers. L is the dummy variable, which equals 0 for Japan, 1 otherwise, but this value is smaller than half of the standard error of 0.29. The L for the relation of Ms was 0.17 (Fukushima and Tanaka, 1990). One possibility for this decrease may be the difference between Ms and Mw; namely, Mw is more common every where.

Photo 3. Surface rupture in Izmit and typical house just beside the fault.

Nevertheless, the comparison should be presented for outside of Japan. Ground conditions at the individual observation sites were not ranked, so this equation may be taken as corresponding to average ground conditions in Japan. The observed PHAs during the 1995 Hyogo-ken Nanbu, Japan earthquake agree well with this attenuation law (Fukushima et al.,2000). Although the law was developed for Japan, we compared it with data from the Kocaeli earthquake. It is applicable to distances up to about 300 km for Mw 7.4. As shown in Figure 7(a), the observed data agree well with the attenuation relation for overseas.

Additionally, observed PHAs from the November 12, 1999 Düzce earthquake (Mw = 7.1) were compared with the attenuation relation as shown in Figure 7(b). Even though Mw of this event was smaller than that of the Kocaeli earthquake, a larger PHA of 805.8 mg was observed at Bolu. This may be due to the large stress drop, forward directivity and/or ground condition at the site.

Comparisons with the regulatory Turkish spectra

The 1998 Turkish seismic design code

The Turkish seismic design code concerning the constructions in seismic areas has been recently modified (Specification for Structures to be Built in Disaster Areas, 1998). It has been implemented since the second of July 1998. We compare the recorded spectra for two largest strong motions of DZC and SKR with the regulatory spectrum.

The spectral acceleration coefficient, A(T), corresponding to 5% damped elastic design acceleration spectrum normalized by the acceleration of gravity, g, is given by equation (2) which shall be considered as the basis for the determination of seismic loads.

$$A(T) = A_0 * I * S(T) \tag{2}$$

Where, T is natural period of the building, $A_0 = 0.40$ (effective ground acceleration coefficient, 0.4 is the value for seismic zone 1 in Turkey), I = 1.0 (building importance factor, value for the standard buildings, hotels, . . .).

Photo 4. Tree split by surface rupture between Izmit bay and Sapanca lake.

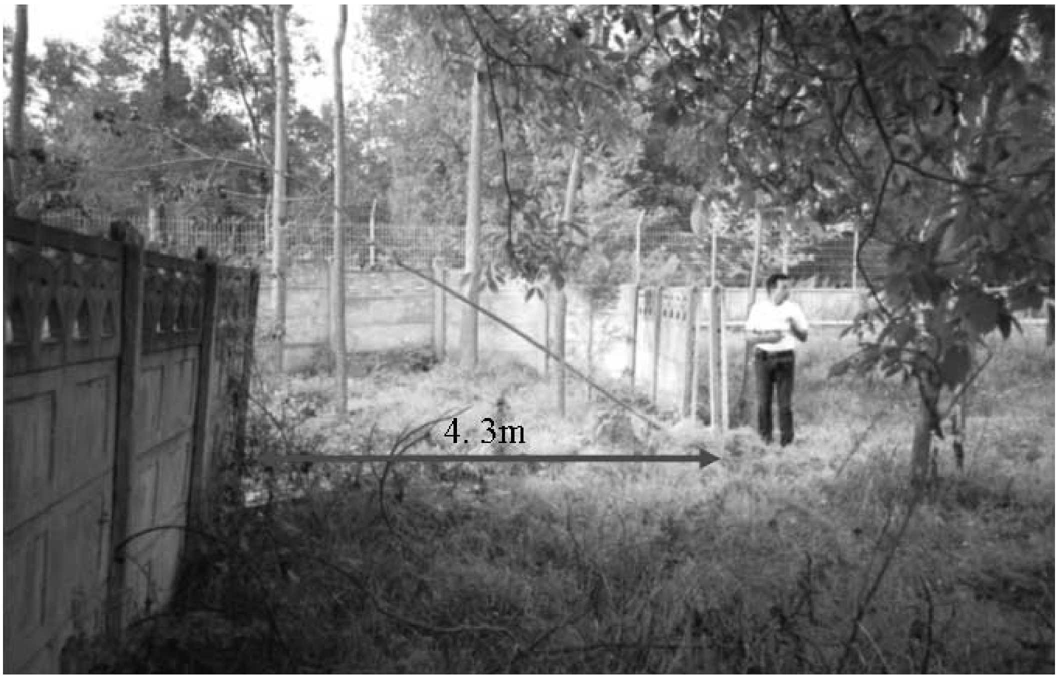

Photo 5. Fence dislocated by surface rupture east of Sapanca lake. The dislocation is 4.3 m.

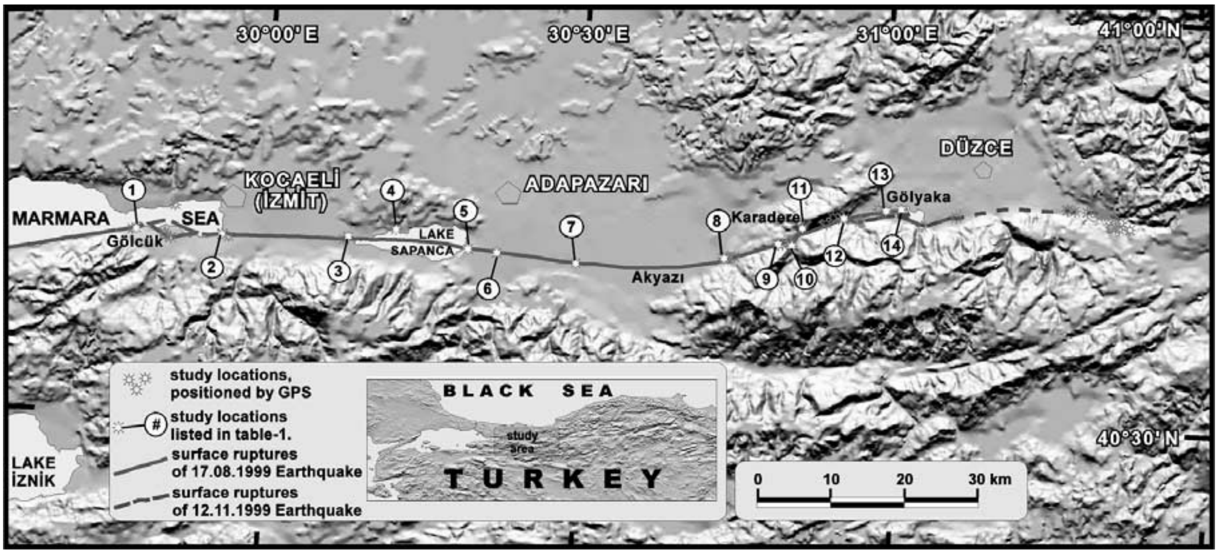

Figure 3. Surface trace of the events on 17 August and 12 November.

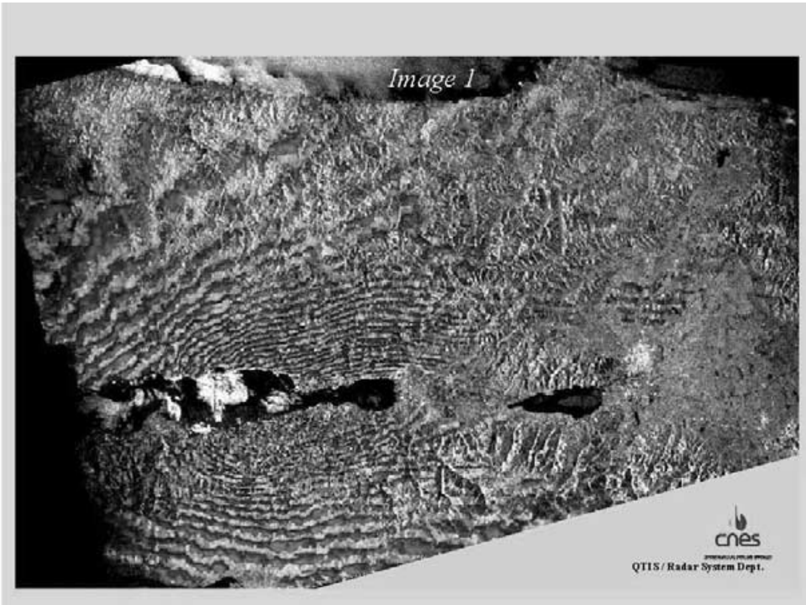

Figure 4. Interferogram from satellite images indicating displacement before and after the event.

S(T) is the spectrum coefficient, appearing in equation (2) and is determined by the following equation (3), depending on the local site conditions and the building natural period, T:

$$S(T) = 1 + 1.5\,T/T_A \quad (0 \leftarrow T \leftarrow T_A) \qquad (3a)$$
$$S(T) = 2.5 \quad (T_A < T \leftarrow T_B) \qquad (3b)$$
$$S(T) = 2.5\,(T_B/T)^{0.8} \quad (T > T_B) \qquad (3c)$$

We used $T_A = 0.1$ s and $T_B = 0.3$ s (spectrum characteristic periods). The choices in the numerical values we used are the least unfavorable. Essentially, we consider a rock spectrum for standard houses.

Elastic seismic loads that are to be determined in terms of spectral acceleration coefficient defined in (2) shall be divided by the seismic load reduction factor (R), defined below, to account for the specific nonlinear behavior of the structural system during the earthquake. In Turkey, R is equal to 4 for conventional buildings.

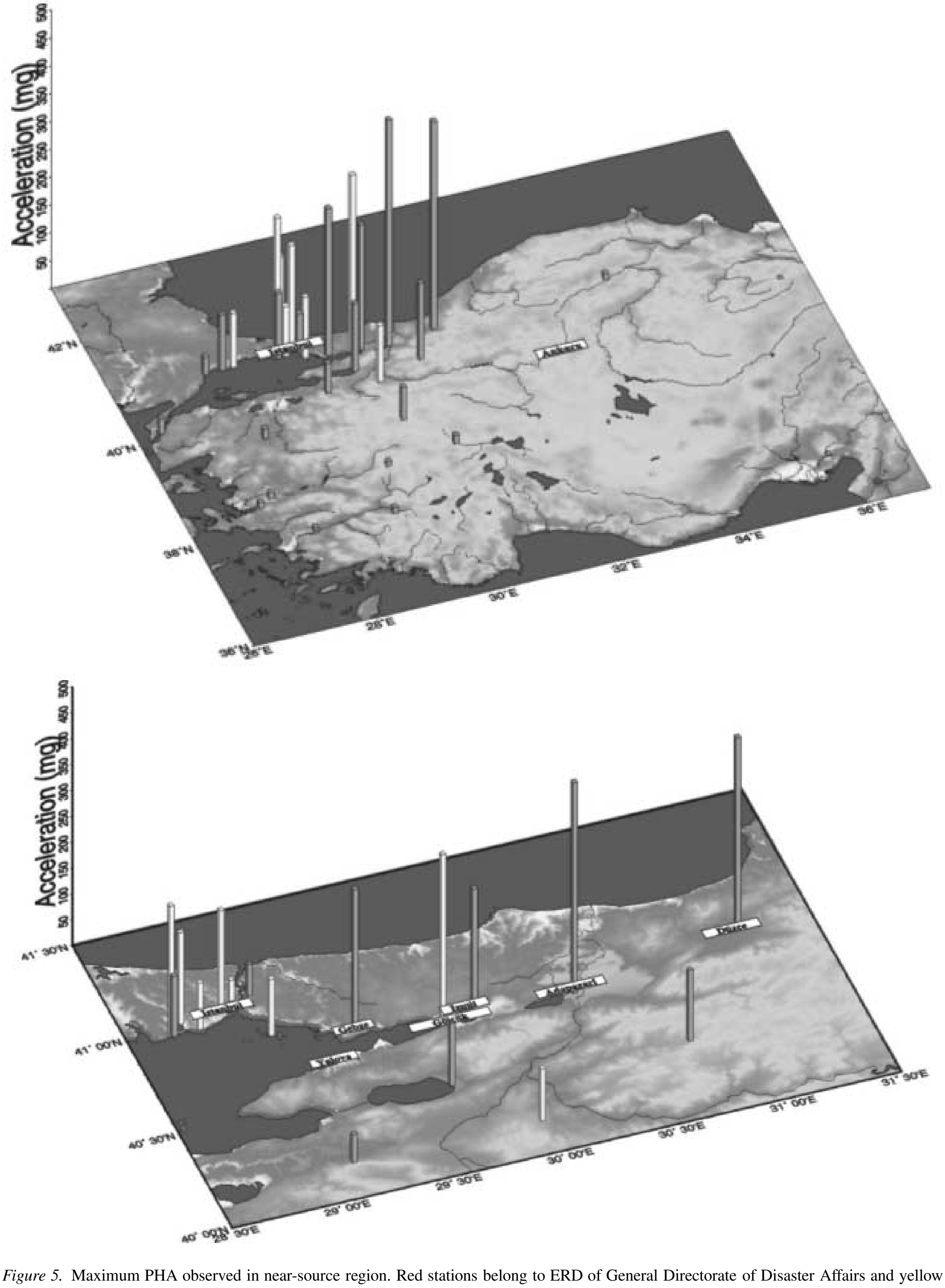

Figure 5. Maximum PHA observed in near-source region. Red stations belong to ERD of General Directorate of Disaster Affairs and yellow ones to Kandilli Observatory & Earthquake Research Institute.

Table 2. Observation station and recorded peak accelerations

(a) Kandilli Observatory & Earthquake Research Institute

Station	Longitude	Latitude	Max PHA (mg)	PVA (mg)	Distance (km)
ATS	28.689	40.975	252.564	80.078	41
CNA	28.755	41.022	177.307	57.678	42
DHM	28.819	40.976	90.210	55.115	36
YKP	29.007	41.075	41.070	27.100	44
YPT	29.800	40.750	322.205	241.089	3
FAT	28.950	41.052	189.392	131.714	42
HAS	29.087	40.868	110.230	143.494	20
BUR	29.970	40.171	100.891	48.218	62

(b) Earthquake Research Department of General Directorate of Disaster Affairs

Station	Longitude	Latitude	PHA EW (mg)	PHA NS (mg)	PVA (mg)	Distance (km)
TKT	36.554	40.328	0.8	1.2	0.4	472
KUT	29.997	39.419	50.0	59.7	23.2	146
AYD	27.838	37.837	5.9	5.2	3.3	333
DNZ	29.114	37.812	5.9	11.7	3.7	322
BRN	27.229	38.455	9.9	10.8	3.3	295
TOS	34.037	41.013	11.7	8.9	4.4	251
CNK	26.402	40.142	24.6	28.6	7.9	231
USK	29.404	38.671	8.9	7.2	3.4	227
BLK	27.860	39.650	17.8	18.2	7.6	150
AFY	30.561	38.792	13.5	15.0	5.0	213
MNS	27.450	38.580	12.5	6.5	4.5	273
BRS	29.131	40.183	54.3	45.8	25.7	57
IST	29.090	41.080	60.7	42.7	36.2	42
SKR	30.384	40.737	–	399.0	259.0	3
TKR	27.515	40.979	32.2	33.5	10.2	129
IZN	29.691	40.437	91.8	123.3	82.3	34
ERG	27.790	40.980	91.4	101.4	57.0	105
CEK	28.700	40.970	118.0	89.6	49.8	40
IZT	29.960	40.790	171.2	221.9	146.4	8
GBZ	29.440	40.820	264.8	141.5	198.5	10
DZC	31.170	40.850	373.7	314.8	470.9	7
GYN	30.734	40.385	117.8	137.7	129.9	35

Seismic load reduction factor, Ra(T), shall be determined by equations (4) in terms of structural behavior factor, R, and the natural vibration period T.

$$Ra(T) = 1.5 + (R - 1.5)\, T / TA \quad (0 \leftarrow T \leftarrow TA) \qquad (4a)$$

$$Ra(T) = R \quad (T > TA) \qquad (4b)$$

So, elastic seismic loads are determined in terms of spectral acceleration coefficient by:

$$Ac(T) = A(T)/Ra(T) \qquad (5)$$

For a null period, the value of Ac is equal to 267 mg.

The 1975 Turkish seismic design code

Because of the recent introduction of the last Turkish code (Specification for Structures to be Built in Disaster Areas, 1998), we decided to compute the regulatory Turkish spectra with the 1975 Turkish seismic design code. Indeed, most of the damaged buildings in the epicentral area were built before 1998. The spec-

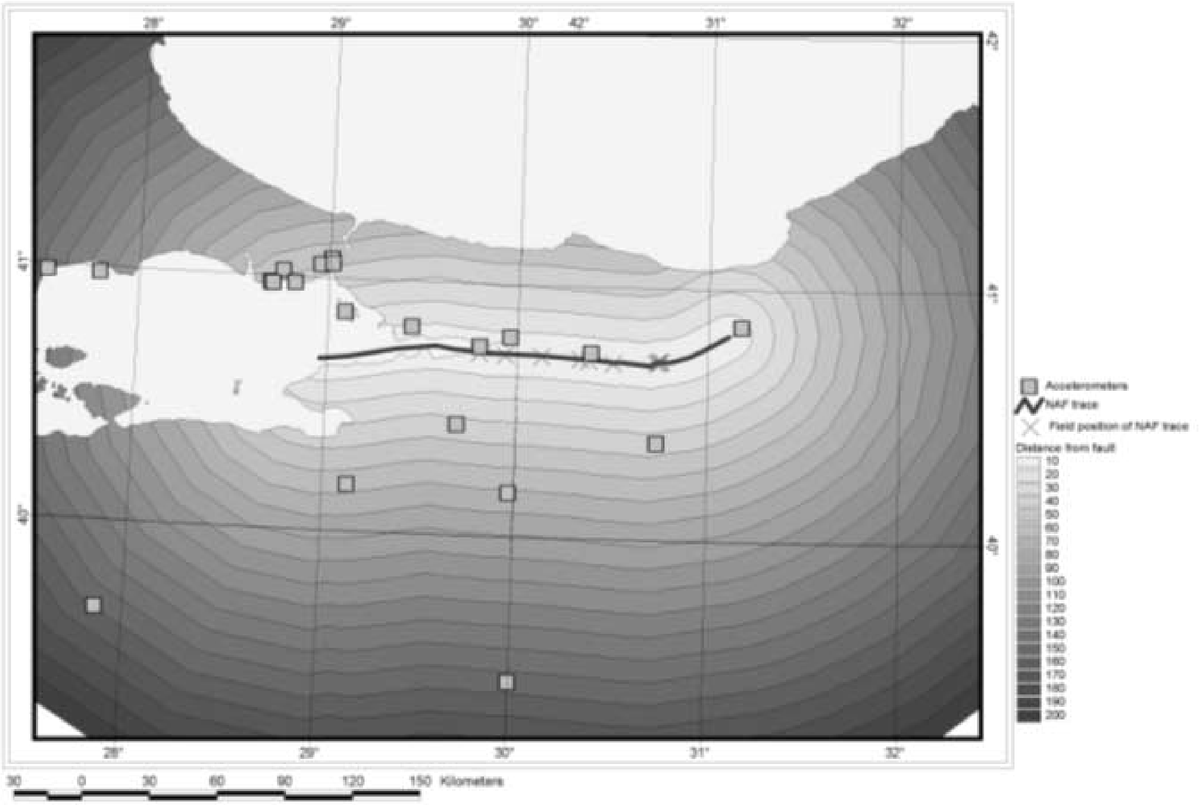

Figure 6. Iso-distance map from approximate point of fault rupture. Points indicate observation stations.

trum corrected from the seismic load reduction factor is given by (6):

$$C(T) = C_0{}^*I^*S(T)^*K \tag{6}$$

Where $C_0 = 0.1$ (value to take into account for the seismic zone 1 in Turkey) and $I = 1.0$ (building importance factor, value for the standard buildings, hotels, ...). $S(T) = 1/(0.8 + T - T_0)$, where T_0 is the predominant period for the soil ($T_0 = 0.25$ s for rock site). K is the structural behavior factor ($K = 1.2$ is a reasonable value for conventional buildings). For a null period, the value of C is equal to 218 mg.

Comparisons

Figure 8 shows that for standard houses (with a resonance period between 0.4 and 1 s), the regulatory spectra (including the behavior factor) are below the spectra computed from the recorded accelerations, for both the 1975 and 1998 codes. Note that the calculation of the spectra for rock conditions do not have an influence on the acceleration for null period, it changes only the duration of the plateau (longer for alluvium conditions). The elastic spectrum (green dashed line) has been computed following the 1998 code (rock spectrum for conventional houses with value for null period equal to 400 mg). The spectra computed from the recorded accelerations are always below the elastic spectrum.

These results show that the spectra computed from the recorded accelerations are below the elastic regulatory spectra. The spectra including the behavior factor are considered as minima to be taken into account by the design engineers. However, all the spectra with behavior factor are always lower than the spectra computed from the recorded accelerations, especially between 0.1 and 1 s. This period range is typical for the resonant period of many buildings. To give an example, an empirical formula gives a rough estimation of the resonant period function of the numbers of floors in the building for concrete frame structures (RPA88): $T_0 = n/10$ (with n the number of floors of the building). During our post-seismic mission in Turkey, we observed that the majority of the buildings had a

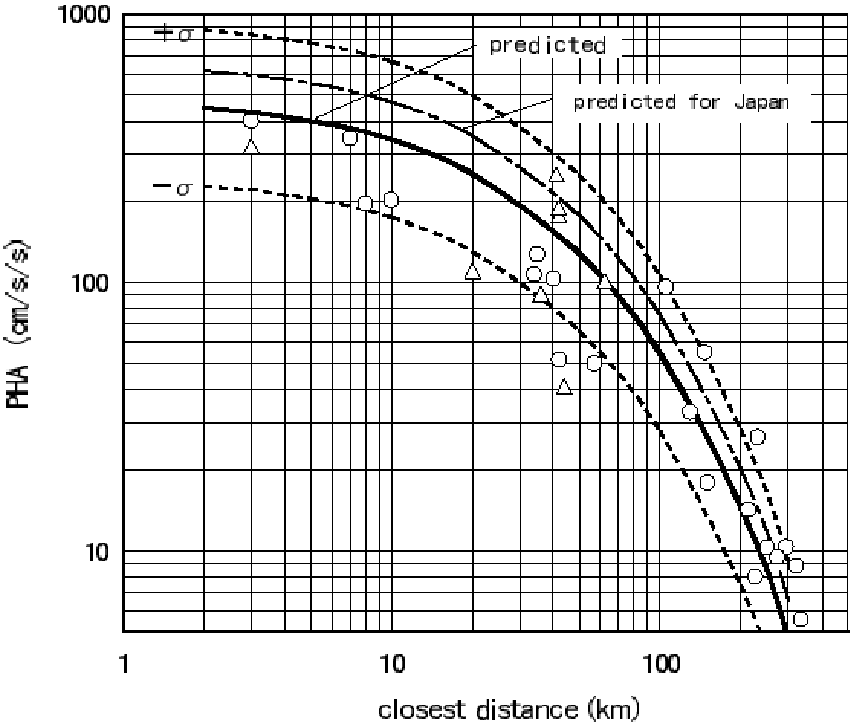

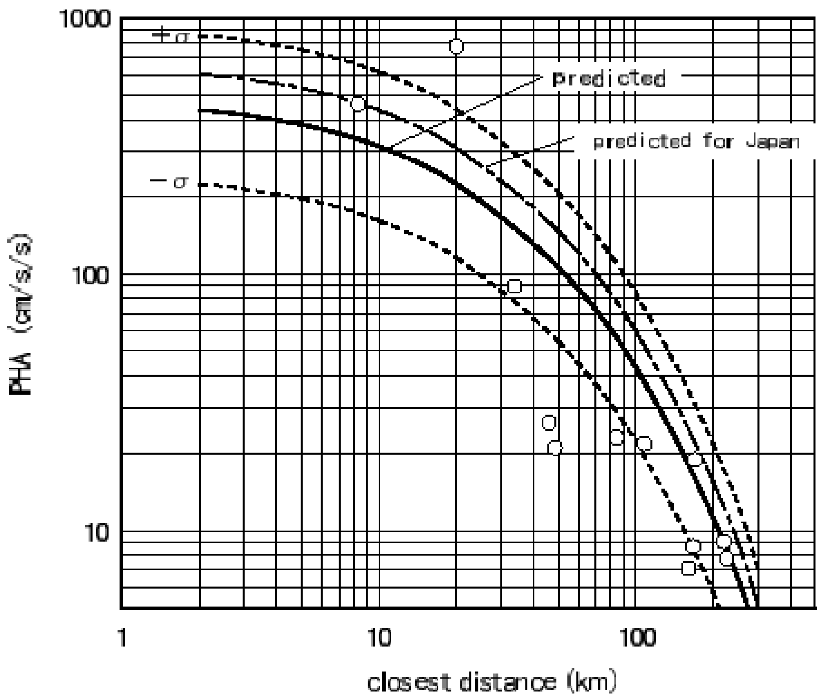

Figure 7. Comparison between observed peak horizontal accelerations and values predicted using empirical attenuation (Equation (1)). Solid line indicates predicted peak horizontal acceleration for overseas. Broken lines indicate the standard error of the equation. Chained line indicates predicted peak horizontal acceleration for Japan. Circles indicate data of Kandilli Observatory and Earthquake Research Institute. Triangles indicate data of Earthquake Research Department of General Directorate of Disaster Affairs. (a) 17 August Kocaeli earthquake, Mw = 7.4, (b) 12 November Düzce earthquake, Mw = 7.1.

Photo 8. Building with accelerometer in Gebze.

Photo 6. Fence dislocated by right lateral movement at eastern end of the fault.

Photo 7. Surface trace at east end of fault rupture at point 14 in Figure 3.

resonant frequency in the range 0.1–1 s (number of floors lower than 10).

The main goal of the spectra incorporating a behavior factor is to be able to design of buildings against collapse, in order to safeguard human life. When the spectra with behavior factor are exceeded during an earthquake, it does not mean that the building designed with this spectrum will collapse, but that the building will no longer behave in the elastic domain: the building will come into the elasto-plastic domain.

The massive destruction observed during the post seismic mission could be due to the quality of con-

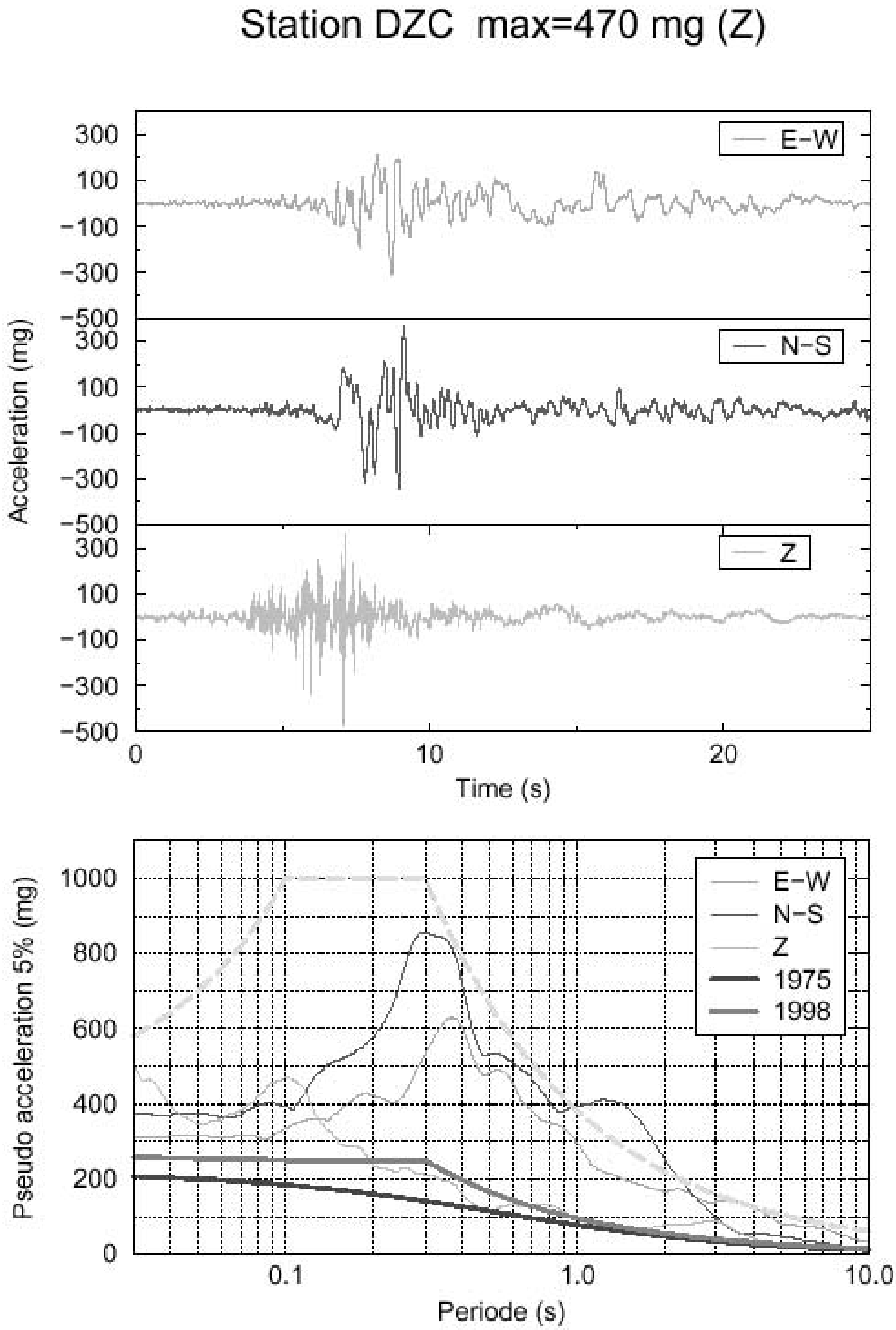

Figure 8. Spectra computed from recorded accelerograms (3 components) for (a) DZC and (b) SKR. The green dashed line represents the elastic spectra derived from the 1998 Turkish code. The spectra including behaviour factor (reduced spectra) are also represented with the 1998 Turkish code (red), and with the 1975 Turkish code (blue).

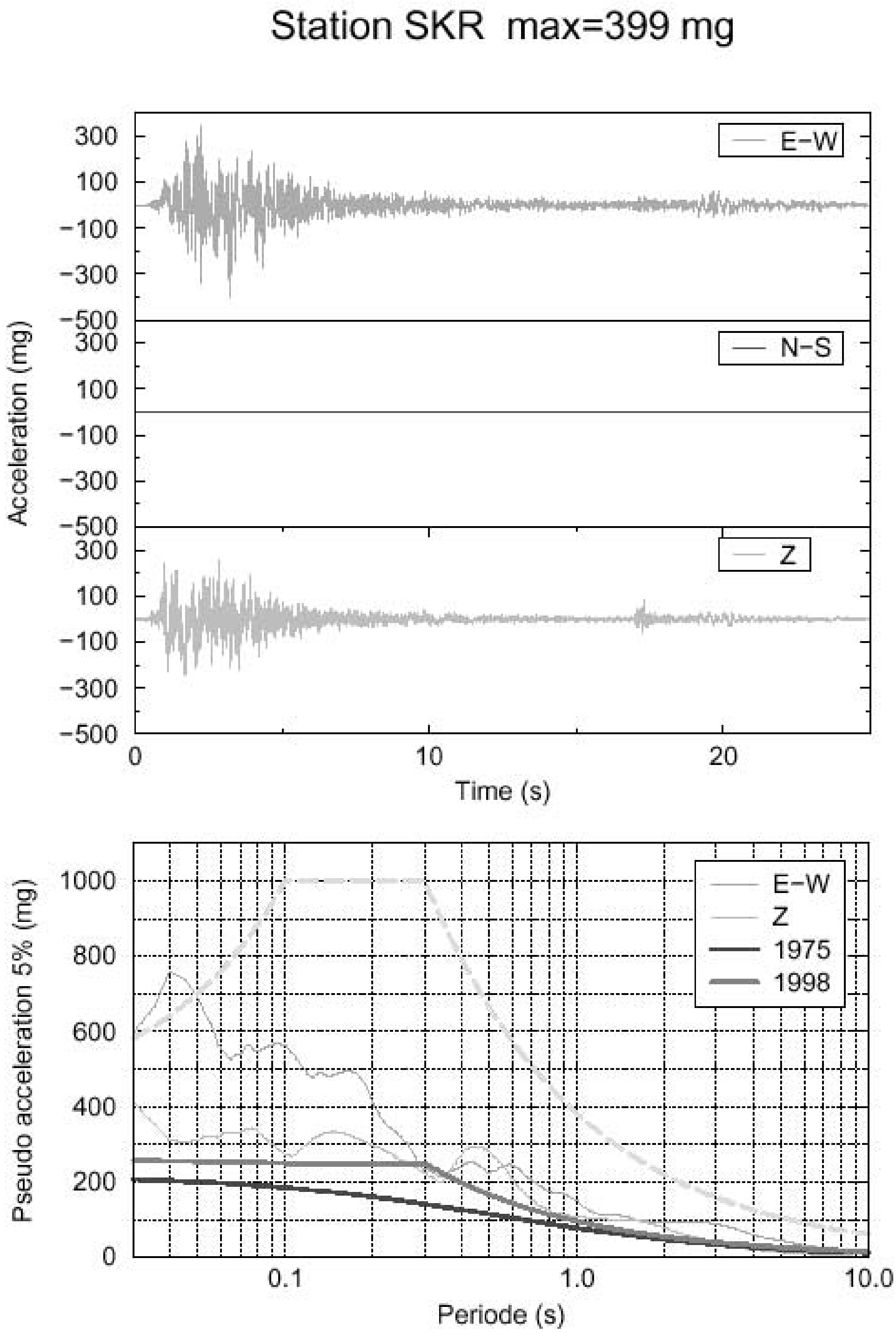

Figure 8. Continued.

Photo 9. Instrument fitted to foundation.

struction, details, quality of material and design (weak-story mechanism, plan eccentricities that have induced torsional response . . .). Moreover, as well as these conception problems, some local uncertainties about soil conditions (site effects, packing down of the soil) probably exist. It is not always easy to take into account these uncertainties during the calculation of spectra with behavior factor. All the observed damage could be due to design and construction problems rather than the definition of spectra with behavior factor.

Discussion

Very severe damage was seen around the source of the Kocaeli earthquake but, paradoxically, many ordinary houses right beside the fault trace survived. Although it should be borne in mind that some of the observation stations are located on better ground conditions than their surroundings, for example on hills (Dr Kagawa; personal communication), the observation record indicates peak ground accelerations of less than 0.5 G. This level is predictable by the simple empirical attenuation relation. We look forward to seeing more accurate investigations of the ground conditions.

In the Gölcük area, large vertical dislocations occurred even though the earthquake mechanism was right lateral slip. As shown in Figure 9, such vertical dislocations arose in the region between two parallel strike slip faults, which has the characteristics of a tensional field because it is between the left-going ground of the north trace and the right-moving ground of the south trace. Just as in the area east of Izmit, the rupture trace jumps suddenly to another line and a vertical downward settlement is seen, even though at a very small scale. It is interesting that rupture initiation took place near these jumps. In the case of the 1995 Hyogo-ken Nanbu earthquake, also, initiation occurred immediately below a jump in the segmentation at the Akashi channel.

As shown in Figure 10, there was a surface break north of Sapanca lake, but we were unable to confirm the right lateral component. To the east and west of the lake, clear right lateral traces were visible, so these may comprise the main rupture strikes under Sapanca lake.

Acknowledgements

We are grateful to the Association Française du Génie Parasismique (AFPS), for giving us the opportunity to be in the scientific commission of the site investigation of the Kocaeli earthquake. We are grateful also to the Ministry of Public Works and Environment (France) who organized the mission of AFPS. Very important support to this organization was provided by the Ministry of Foreign Affairs of France, Embassy of France in Turkey and Embassy of Turkey in France. We have the pleasure to acknowledge to Prof. Mustafa Erdik, chairman of Earthquake Engineering Division, Kandilli Observatory & Earthquake Research Institute (KOERI) of Bogaziçi University, Turkey, who organized a briefing for us. We also acknowledge all the other Turkish people, who kindly gave us information during our field investigations in the region.

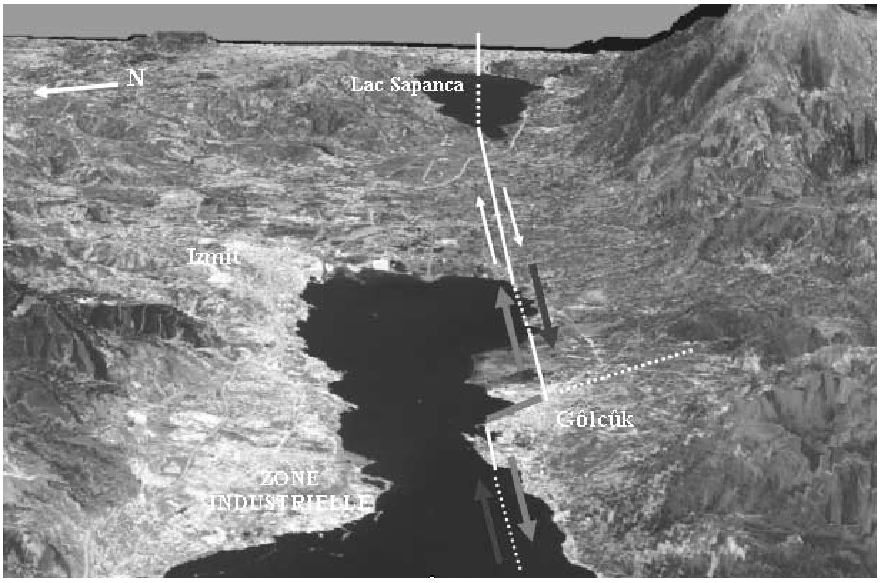

Figure 9. Bird's-eye view of Izmit area and approximate location of surface ruptures.

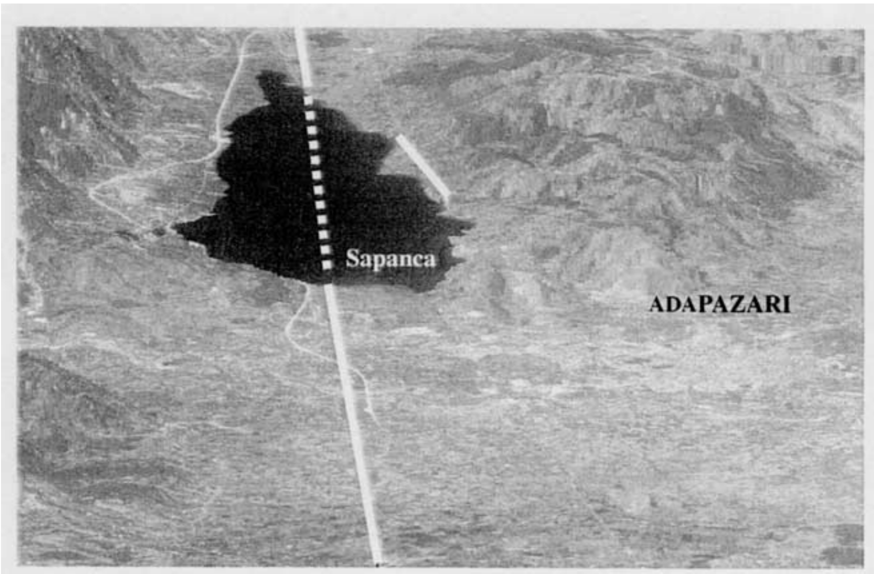

Figure 10. Bird's-eye view of Sapanca lake area.

References

Fukushima, Y. and Tanaka, T., 1990, A new attenuation relation for peak horizontal acceleration of strong earthquake ground motion in Japan, *Bull. Seism. Soc. Am.* **80**, 757–783.

Fukushima, Y. and Tanaka, T., 1992, Revised attenuation relation of peak horizontal acceleration by using a new data base. Programme and Abstracts, *SSJ* **2**, 116. (in Japanese)

Fukushima, Y., Irikura, K., Uetake, T. and Matsumoto, H., 2000, Characteristics of observed peak amplitude for strong ground motion from the 1995 Hyogo-ken Nanbu (Kobe) earthquake, *Bull. Seism. Soc. Am.* **90**, 545–565.

Kagawa, T., 1999, Strong ground motion simulation due to the 1999 Kocaeli earthquake, Turkey. Programme and Abstracts, *SSJ* **A73**. (in Japanese)

Kasapoglu, K.E., Ulusay, R., Gökçeoglu, C., Sönmez, H., Binal, A. and Tuncay, E., 1999, 17 Agustos 1999 Dogu Marmara depreminin jeoteknik saha inceleme raporu, Hacettepe Univ., Fac. of Eng., Dept. of Geol. Eng., Applied Geology Subdivision, p. 95, Beytepe, Ankara, Turkey.

Koketsu, K. and Komiyama, H., 1999, Directivity effect on strong motion and teleseismic seismograms from the 1999 great Turkey earthquake. Programme and Abstracts, *SSJ* **A72**. (in Japanese)

Kudo, K., Kanno, T., Okada, H., Özel, O. and Erdik, M., 1999, Site specific surveys at strong motion observation sites and damaged areas from the Kocaeli, Turkey earthquake of August 17, 1999. Programme and Abstracts, *SSJ* **A75**.

Régles Parasismiques Algériennes, 1988, Centre National de Recherche Appliquée en Génie Parasismiques, Alger, Algérie, **RPA88** (in French).

Sekiguchi, H. and Iwata, T., 1999, Source process of the 1999 Kocaeli, Turkey earthquake estimated from strong ground motion waveforms. Programme and Abstracts, *SSJ* **A71**. (in Japanese)

Yagi, Y. and Kikuchi, M., 1999, Source process of 17 August 1999 Turkey earthquake. Programme and Abstracts, *SSJ* **A70**. (in Japanese)

Youd, T.L., Bardet, J.P. and Bray, J.D. (eds), 2000, Kocaeli, Turkey, Earthquake of August 17, 1999 Reconnaissance Report, *Earthquake Spectra* **16**(Suppl. A).